INVESTIGATION OF SEPARATION CONTROL FOR LOW-PRESSURE TURBINES USING CFD

Hermann F. Fasel*, Wolfgang Balzer*, Andreas Gross*
***University of Arizona, Tucson, AZ 85721, USA**

Keywords: *Low-pressure turbine (LPT), computational fluid dynamics (CFD), active flow control (AFC), direct numerical simulation (DNS), vortex generator jets (VGJ)*

Abstract

Separation from low-pressure turbine (LPT) blades at low operating Reynolds numbers can significantly degrade performance. We investigated separation control by steady and pulsed vortex generator jets (VGJs) as well as harmonic blowing through a spanwise slot using computational fluid dynamics (CFD). The detailed fluid dynamics were explored in fully resolved direct numerical simulations (DNS) for a flat and curved plate model geometry under LPT conditions. The most promising AFC control schemes were then validated for the full LPT blade geometry. Steady VGJs were found to generate streamwise vortices. Our simulations have shown that pulsed VGJ actuation leads to an earlier transition to turbulence and the generation of spanwise coherent structures. In both cases, separation is controlled by an increased entrainment of freestream fluid. The stunning effectiveness of pulsed VGJs is explained by a hydrodynamic instability mechanism which amplifies spanwise instability modes.

1 Introduction

The low-pressure turbine (LPT) is an important element of modern jet engines. Low-Reynolds number operating conditions and aggressive blade designs can lead to laminar separation which is highly undesirable as it can result in significant reductions in turbine and overall engine performance. Prediction and control of LPT separation, without sacrificing the benefits of higher blade loading, are therefore crucial for improved engine designs.

In experiments, Bons et al. [1] and Sondergaard et al. [2] systematically explored the potential advantages of active flow control (AFC) using vortex generator jets (VGJs) for LPT separation control. Both, steady and pulsed VGJs were reported to be effective in reducing separation losses. However, pulsed blowing was shown to be much more efficient, requiring only a small fraction of the mass flow rate when compared to steady VGJs. Pulsed blowing was shown to cause early boundary layer transition, especially when the jets were employed near the "natural" (uncontrolled) separation location [1].

In this paper a short summary of our numerical investigations of AFC for LPT separation control is provided. The chord Reynolds number based on axial chord length, C_x, and inlet velocity, v_∞, was Re=25,000. We first investigated the relevant fluid dynamics of VGJ flow control for a flat and curved plate model geometry under LPT conditions using fully resolved direct numerical simulations (DNS) [3-5]. We then validated the most promising AFC strategies for a full LPT geometry, the Pratt and Whitney Pack B LPT blade [6,7].

2 Numerical Methods

For the model geometry simulations we use a highly efficient finite-difference code based on the incompressible Navier-Stokes equations in vorticity-velocity formulation [8] which has been adopted for curvilinear grids [9]. The current version of the code employs fourth-order-accurate compact finite differences in combination with a fourth-order-accurate explicit Runge-Kutta time integration. The spanwise direction is treated with a pseudo-

spectral approach, which results in very high accuracy. For simulations of the full geometry we employ a finite-volume code based on the compressible Navier-Stokes equations in curvilinear coordinates [10]. The code is based on a ninth-order-accurate upwind scheme for the convective terms, a fourth-order-accurate discretization for the viscous terms, and the second-order-accurate implicit Adams-Moulton method for time integration.

3 Grid and Boundary Conditions

A schematic of the computational domain for the flat plate model is shown in Fig. 1. A laminar boundary layer profile is prescribed at the inflow boundary. The separation bubble is generated by specifying an appropriate boundary condition for the normal velocity component at the upper boundary so that a pressure gradient for the LPT conditions is imposed. Near the outflow boundary a buffer domain is employed which acts as a sponge and dampens flow structures. Flow periodicity is enforced in the spanwise direction. The domain width was 13.5% of the axial chord length, C_x. The setup for the curved plate simulations is identical. The typical number of grid points for the model geometry simulations was in the range of 10^7 and up to $165 \cdot 10^6$.

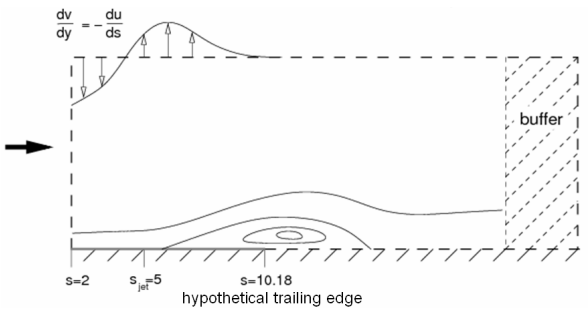

Fig. 1. Schematic of computational domain for flat-plate model.

For the simulations of the full geometry we employed a body-fitted grid consisting of 5 blocks. The wall was treated as adiabatic and a characteristics based boundary condition was employed at the inflow and outflow boundaries. The spanwise domain width was $0.2C_x$ and flow periodicity was enforced in the spanwise direction. The number of grid points was in the order of 10^7.

4 Results

4.1 Flat Plate Simulations

We first considered the uncontrolled flow for the flat plate model geometry. An instantaneous visualization of spanwise vorticity as well as streamlines for the time-averaged flow are shown in Fig. 2. The boundary layer separates at s=5.7 and reattaches in the mean at s=16.8. The arc-length, s, was measured from the leading edge of the blade and non-dimensionalized with $1/7C_x$. The wall-bounded free shear layer associated with the separated boundary layer is subject to a Kelvin-Helmholtz instability which amplifies disturbances and leads to a "roll up" of the shear layer into spanwise vortices (or "rollers") which is followed by transition to turbulence. Interestingly, two-dimensional (2D), spanwise coherent structures are seen to reside in the turbulent flow. Considering that the trailing edge of the LPT blade is at s=10.18 the flow would not reattach to the blade.

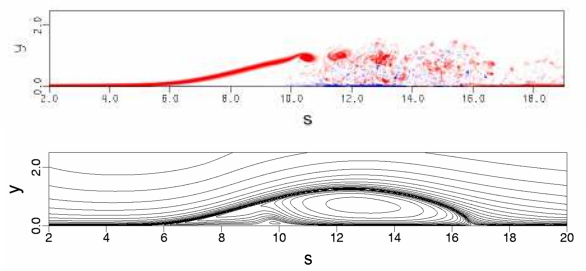

Fig. 2. Uncontrolled flow. Spanwise vorticity (top) and streamlines (bottom).

We first investigated separation control with steady VGJs and both, wall-normal and angled (90° skew and 30° pitch angle) injection. Instantaneous flow visualizations using the λ_2 vortex identification criterion by Jeong and Hussain [11] for blowing ratios of B=1 and 2 are shown in Fig. 3. The blowing ratio is defined as the ratio of jet exit velocity to the freestream velocity, v_∞. Reverse flow regions of the time-mean flow are shaded red. For a blowing ratio

of B=1 little difference is seen between the results with angled and vertical injection. Transition is preceded by the appearance of hairpin like vortex loop structures downstream of the VGJ holes. For B=2 and vertical injection a strong horseshoe vortex develops that "wraps around" the column of fluid injected by the jet. Vortex loop structures evolve in between the two legs of the horseshoe structure. For angled injection the oncoming boundary layer is diverted in the direction of the jet injection and two pronounced streamwise vortices are generated. Compared with the vertical injection, the streamwise vortices maintain their coherence over a longer downstream distance and the laminar-turbulent transition process is delayed. In summary, the primary control mechanism appears to be the entrainment of freestream fluid by steady streamwise vortices.

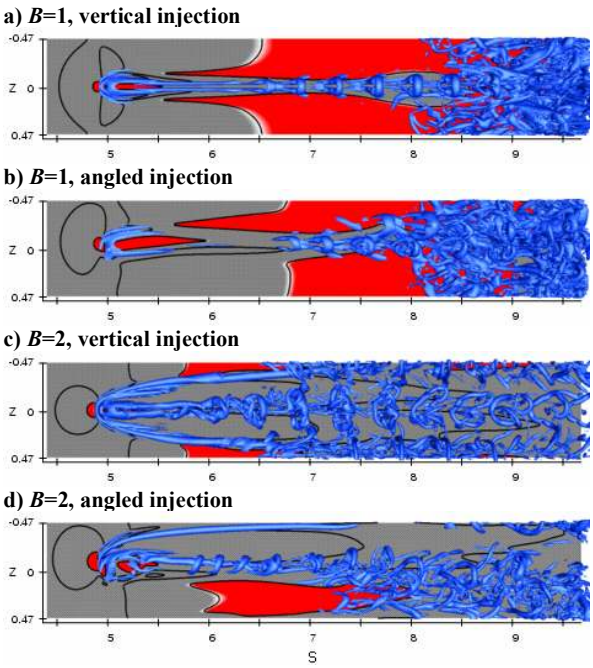

Fig. 3. Iso-surfaces of λ_2=-50 and spanwise wall vorticity for steady VGJs.

The main motivation behind our research was to investigate and explain why pulsed VGJs were so much more effective than steady VGJs. Results from a typical simulation are shown in Fig. 4. The VGJs were pulsed with a frequency of f=5.4 (non-dimensionalized with v_∞ and C_x), a blowing ratio of B=1, and a duty cycle (ratio of jet on time to forcing period) of τ=10%. Compared with the uncontrolled flow pulsed VGJ actuation resulted in an earlier transition. More important, and surprising at first, the simulations also revealed that for both, vertical and angled injection, strong spanwise coherent vortical structures developed in the separated flow region. This observation led to the conjecture that the formation of these spanwise coherent structures may be the primary cause for the increased effectiveness of pulsed VGJ actuation versus steady VGJs.

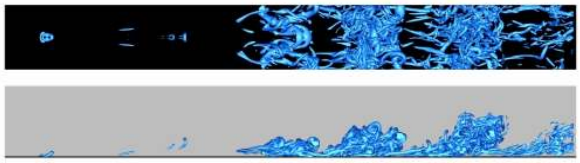

Fig. 4. Iso-surfaces of λ_2=-25 for pulsed vertical VGJs with f=5.4, B=1, and τ=10%.

A proper orthogonal decomposition (POD) [12,13] of the time-dependent flow data confirmed this conjecture. For the same case with vertical injection, POD mode 1, which contains most of the unsteady kinetic energy, is shown in Fig. 5. Since modes 1 and 2 represent the spanwise coherent structures and since the corresponding POD time signals were in perfect phase with the pulsed actuation we conjectured that the similar effectiveness of angled and vertical jets must be due to the unsteady (periodic) "in phase" pulsing which introduces 2D disturbances.

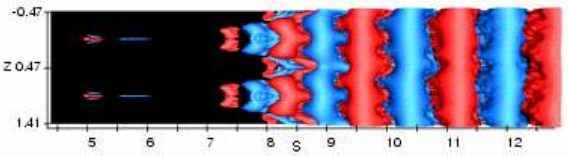

Fig. 5. POD mode 1 (iso-surfaces of |v| = 0.025) for pulsed vertical VGJs with f=5.4, B=1, and τ=10%.

Due to the shear layer instability of the separated boundary layer these 2D disturbances undergo a strong amplification in downstream direction leading to the formation of the aforementioned large-scale spanwise coherent structures. A plot of the 2D velocity disturbance amplitude versus the downstream coordinate is shown in Fig. 6. After a transient, downstream of the exit holes (the jets are located at s=5), the

2D disturbances experience approximately exponential growth which is an indication of a linear instability mechanism. Because a linear instability mechanism is exploited, the energy required for the amplification of the 2D disturbances is provided by the base flow and comes "free of charge". The streamwise vortices generated by steady VGJs are not amplified by the flow. This difference explains the greater effectiveness of pulsed VGJs when compared with steady VGJs.

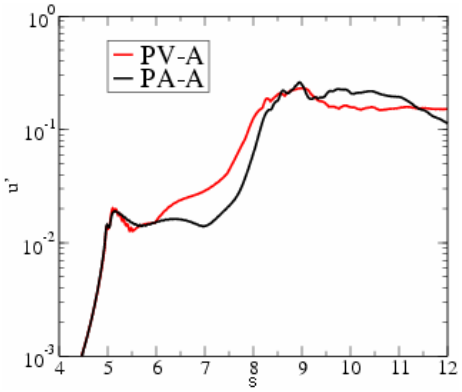

Fig. 6. Fourier amplitude of the 2D component of the *u*-disturbance velocity (max. over *y*) for pulsed vertical and angled VGJs.

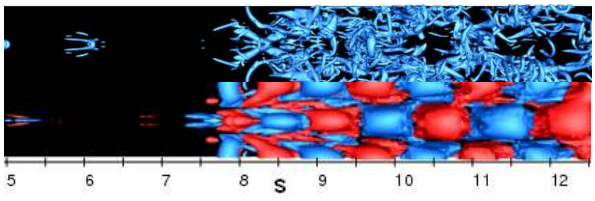

Fig. 7. Pulsed vertical VGJs with f=5.4, B=1, and τ=40%. Iso-surfaces of λ_2=-25 and POD mode 1 (iso-surfaces of |v| = 0.025).

Simulations where we varied the duty cycle, τ, indicated that the duty cycle had no significant effect on the effectiveness of the VGJ separation control. Rather, besides the blowing ratio, the unsteady "in phase" actuation and the forcing frequency were found to be important parameters. This was seen as additional confirmation that the exploitation of an underlying 2D instability mechanism was essential for an effective VGJ separation control. From an engineering point of view lower duty cycles are preferable as they require smaller mass fluxes and thus less energy. Instantaneous flow visualizations and results obtained from a POD analysis of the flow data (Fig. 7) reveal that, for intermediate duty cycles (here: τ=40%), the flow structures are concentrated in areas with oblique coherence. We conjectured that the amplification of 3D instability modes may lead to the formation of oblique coherent structures.

4.2 Curved Plate Simulations

Results for the curved wall geometry confirmed our findings for the flat plate geometry (Fig. 8). Again, compared to the uncontrolled flow, pulsed VGJs were found to result in an earlier transitioning and the appearance of spanwise coherent structures that were amplified by the flow. Compared to the flat plate, we noticed a higher amplification of the spanwise structures but also an earlier loss of spanwise coherence of these 2D structures in downstream direction due to the stronger amplification of three-dimensional (3D) modes.

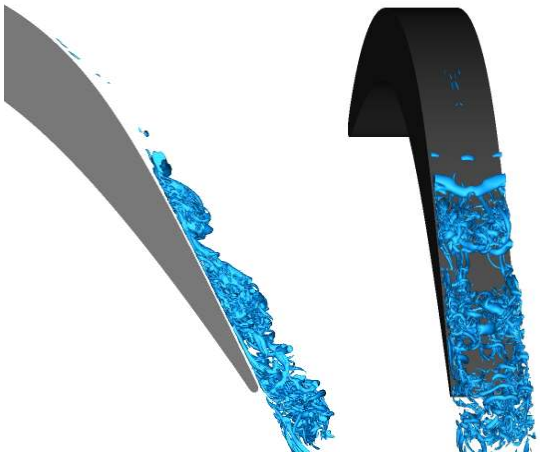

Fig. 8. Iso-surfaces of λ_2=-25 for pulsed vertical VGJs with f=5.4, B=1, and τ=10%.

We also varied the hole spacing and the spanwise domain width. The hole spacing in our earlier simulations was 6D, where D is the hole diameter. A narrower hole spacing results in a larger 2D and a reduced 3D disturbance input, resulting in more prominent 2D spanwise coherent structures and a delayed transition (Fig. 9). In the extreme, for pulsed blowing through a spanwise slot, the flow is dominated by large-amplitude laminar spanwise vortical structures and transition is delayed until far

downstream of the trailing edge. It appears that for this case, the secondary instability mechanism that results in the amplification of 3D disturbances is weakened.

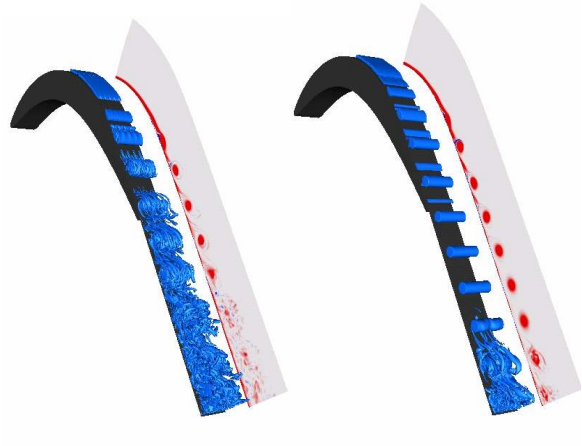

Fig. 9. Iso-surfaces of λ_2=-25 and iso-contours of spanwise vorticity for pulsed vertical VGJs (f=5.4, B=1, and τ=10%, and hole spacing 2D, left) and forcing through slot (right).

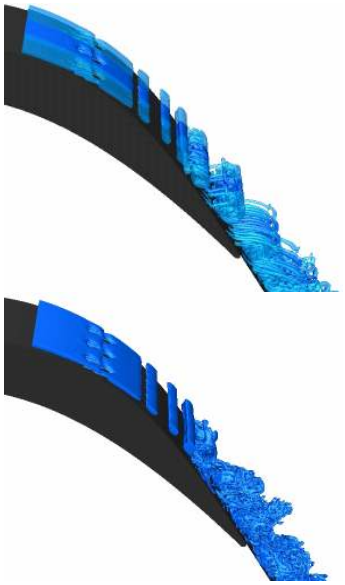

Fig. 10. Iso-surfaces of λ_2=-25 for pulsed vertical VGJs (f=5.4, B=1, and τ=10%, and hole spacing 2D) for domain width of 2D (top) and 6D (bottom).

In addition, we investigated how the spanwise domain extent used in the simulations affected the flow. Results for a hole spacing of 2D and a spanwise domain width of 2D and 6D are shown in Fig. 10. The narrow domain result was repeated twice in the spanwise direction to allow for an easier comparison. For the narrow domain, structures with a spanwise wavelength larger than 2D are suppressed which results in a delayed transition and increased coherence of the spanwise structures compared to the wide domain results.

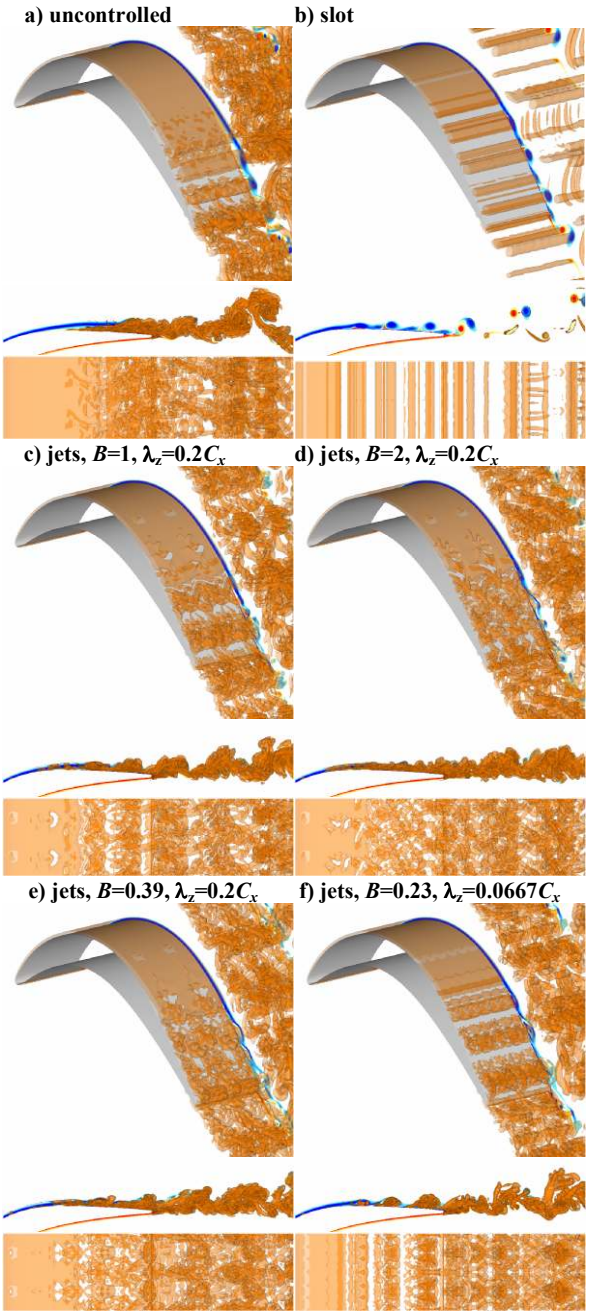

Figure 11. Perspective view, side view, and top view showing iso-surfaces of Q=1.

4.3 Simulations of Entire Geometry

Since the model geometry simulations did not account for the trailing edge, wake, and circulation, we also investigated separation control for the full LPT blade geometry. We considered pulsed angled VGJs with f=5 and τ=10%, wall-normal VGJs with harmonic blowing with f=5, and harmonic blowing through a slot with f=5 and B=0.1. The VGJ hole spacing, λ_z/C_x, was 0.2 and 0.667.

Instantaneous flow visualizations using the Q vortex identification criterion [14] are shown in Fig. 11 (the data were repeated once in the spanwise direction). The uncontrolled flow is seen to transition near the trailing edge and the wake turbulence appears to be concentrated in "lumps". In agreement with the model geometry results, pulsed angled VGJ actuation with B=1 leads to the formation of pronounced spanwise coherent structures. For B=2 the flow appears to transition earlier. As for the curved wall model geometry, for harmonic wall-normal VGJ injection a reduction of the hole spacing results in an increased 2D coherence of the spanwise structures. With harmonic blowing through a spanwise slot the flow relaminarizes and separation is effectively controlled by laminar spanwise vortices.

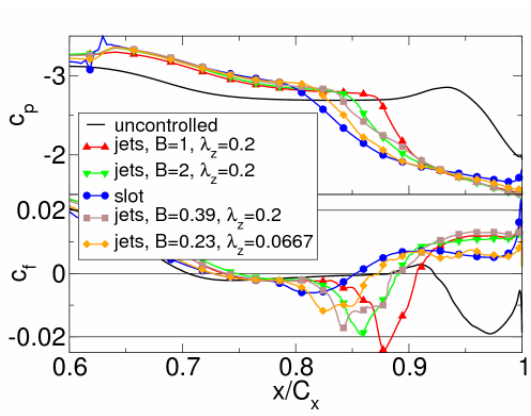

Fig. 12. Wall pressure coefficient, c_p, and skin friction coefficient, c_f.

A comparison of the wall pressure and skin friction distributions is shown in Fig. 12. The uncontrolled flow separates near 70% chord and does not reattach. The separated flow region can be associated with a "pressure plateau". With AFC the length of the separated flow region is reduced significantly. The slot forcing and the VGJs with λ_z/C_x=0.0667 and B=0.23 are most effective.

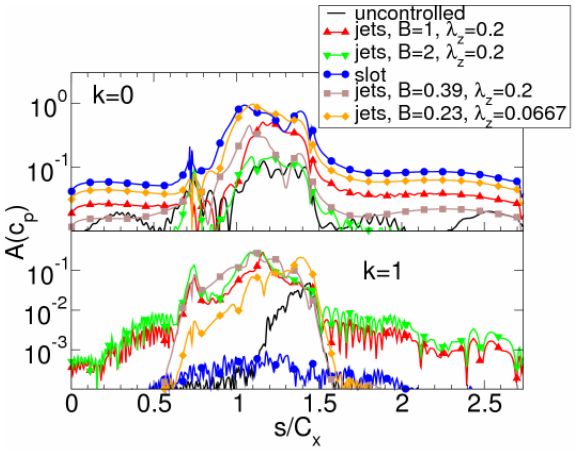

Fig 13. Wall pressure coefficient disturbance amplitudes for fundamental (f=5) and spanwise modes k=0 and 1.

Finally, amplitude distributions of the f=5 and k=0 (spanwise average) and k=1 (first spanwise Fourier mode) disturbance amplitudes of the wall pressure coefficient are shown in Fig. 13. For harmonic VGJs with λ_z/C_x=0.0667 and B=0.23 and harmonic blowing through a slot the k=0 mode experiences linear amplification beginning roughly at s=0.8C_x. Around $s \approx C_x$ saturation is reached. The linear (exponential) amplification in combination with the two-dimensionality of the flow (the 3D mode k=1 remains essentially zero for the slot) explain the superior effectiveness of this flow control. With pulsed VGJs and B=1, linear growth of the 2D mode is also observed, starting, however, later and from a lower amplitude level and reaching saturation farther downstream compared to the case with slot forcing. As the blowing ratio was smaller for the slot forcing it can be concluded that the introduction of a 2D disturbance which is amplified by the flow and the suppression of 3D disturbances which reduce 2D coherence are essential for an effective separation control. This is in agreement with the model geometry results.

5 Conclusions

We investigated separation control for low-pressure turbine (LPT) blades using computational fluid dynamics (CFD). Steady vortex generator jets (VGJs) were found to generate streamwise vortices which entrain freestream fluid. The vortices are not amplified by the flow and, consequently, large VGJ blowing ratios (and thus a large energy input) are required for obtaining vortices with sufficient strength. Pulsed VGJs were shown to result in an earlier transition of the flow. However, even more important, the pulsed "in phase" actuation was also shown to lead to the formation of spanwise coherent structures which very effectively entrained freestream fluid. The spanwise structures were found to be generated by the flow through a Kelvin-Helmholtz type instability mechanism. Because the energy required for the amplification of the relevant 2D instability modes is provided by the mean flow, pulsed VGJs require lower blowing ratios and are more efficient than steady VGJs. The most effective separation control was achieved for very closely spaced VGJs or blowing through a spanwise slot. In this case transition to turbulence was delayed and the flow was dominated by essentially laminar spanwise vortices.

Acknowledgments

This work was performed under sponsorship from the Air Force Office of Scientific Research, with Dr. T. Beutner, R. Jefferies, and Dr. J. Schmisseur serving as project managers.

References

[1] Bons J, Sondergaard R and Rivir R. The Fluid Dynamics of LPT Blade Separation Control Using Pulsed Jets. *J. of Turbomachinery*, Vol. 124, No. 1, pp 77-85, 2002.

[2] Sondergaard R, Bons J and Rivir, R. Control of Low-Pressure Turbine Separation Using Vortex Generator Jets. *J. of Propulsion and Power*, Vol. 18, No. 4, pp 889-895, 2002.

[3] Postl D, Gross A and Fasel H. Numerical Investigation of Active Flow Control for Low-Pressure Turbine Blade Separation. *AIAA paper* AIAA-2004-0750, 2004.

[4] Postl D. Numerical Investigation of Laminar Separation Control Using Vortex Generator Jets. *PhD dissertation*, University of Arizona, Tucson, 2005.

[5] Balzer W, Gross A and Fasel H. Active Flow Control of Low-Pressure Turbine Separation. *Proceedings of the HPCMP Users Group Conference 2007*, Pittsburgh, PA, editor: D.E. Post, pp 73-82, 2007.

[6] Gross A and Fasel H. Numerical investigation of low-pressure turbine blade separation control. *AIAA J.*, Vol. 43, No. 12, pp 2514-2525, 2005.

[7] Gross A and Fasel H. Investigation of Low-Pressure Turbine Separation Control. *AIAA paper* AIAA-2007-520, 2007.

[8] Meitz H and Fasel H. A Compact-Difference Scheme for the Navier-Stokes Equations in Vorticity-Velocity Formulation. *J. of Comp. Physics*, Vol. 157, No. 1, pp 371-403, 2000.

[9] Postl D and Fasel H. Direct Numerical Simulation of Turbulent Flow Separation from a Wall-Mounted Hump. *AIAA J.*, Vol. 44, No. 2, pp 263-272, 2006.

[10] Gross A and Fasel H. High-Order-Accurate Numerical Method for Complex Flows. *AIAA J.*, Vol. 46, No. 1, pp 204-214, 2008.

[11] Jeong J and Hussain F. On the identification of a vortex. *J. of Fluid Mechanics*, Vol. 285, pp 69-94, 1995.

[12] Lumley, J. The Structure of Inhomogeneous Turbulent Flows. *Atmospheric turbulence and radio wave propagation*, Nauka, Moscow and Toulouse, France, eds. A.M. Yaglom and V.I. Tatarsky, pp 166-178, 1967.

[13] Sirovich L. Turbulence and the Dynamics of Coherent Structures. *Quarterly of Applied Mathematics*, Vol. XLV, No. 3, pp 561-590, 1987.

[14] Hunt J, Wray A and Moin P. Eddies, stream, and convergence zones in turbulent flows. Report CTR-S88, Center For Turbulence Research, Stanford, California, 1988.

Copyright Statement